Self-Powered Broadband Photodetectors: Unveiling the PyroPhototronic Effect and Binary Photoresponse in Different Dimensional Hybrid Structures

Mahesh Kumar, Adhimoorthy Saravanan*, Sheng-Chi Chen*, Bohr-Ran Huang*

4th PhD student, * Advisor

Graduate Institute of Electro-Optical Engineering, National Taiwan University of Science and Technology, Taipei 106, Taiwan

Abstract

The research explores several innovations: a pyroelectric-effect-based hybrid heterostructure of 1D SnO2 nanoneedles and 2D SnS2 nanoflowers, demonstrating remarkable increases in transient and pyroelectric currents across various wavelengths. A novel bidirectional photo response of 0-D C60/2-D SnS2 nanoflower heterostructure for self-powered broadband photodetector. Furthermore, by adjusting the wavelength of the incident light, controllable bidirectional photoresponse (negative for λ = 365 nm and positive for λ = 456, 532, 632, and 850 nm) is achieved through the construction of hole or electron carrier transmission mechanisms. Lastly, a superconductor-semiconductor mixed structure featuring 2D NbSe2/1D ZnO nanorods shows a 1000-magnitude improvement in the photo-to-dark current ratio.

Research Focus

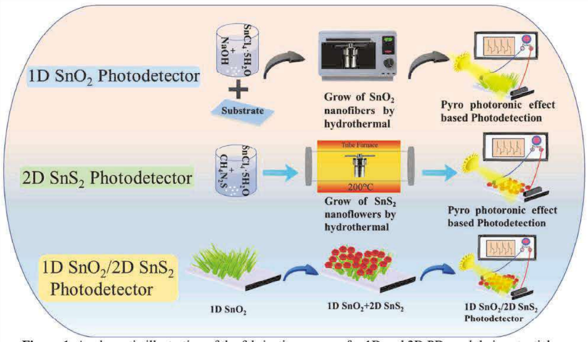

Figure 1. A schematic illustration of the fabrication process for 1D and 2D PDs and their potential use as a PPE-based photodetection performance.

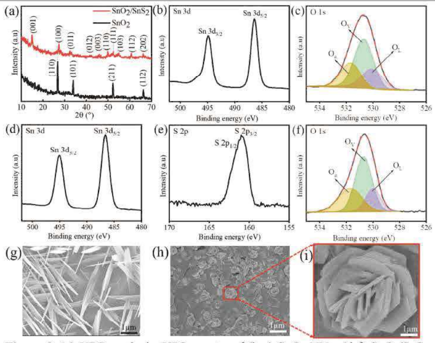

Figure 2. (a) XRD analysis. XPS spectra of (b-c) SnO_2 NNs, (d-f) SnO_2/SnS_2. (g) FESEM image of SnO_2 NNs. (h-i) FESEM image of SnO_2/SnS_2.

Figure 3. Impact of illumination intensities on the PPE. (a-d) determine to short-circuit photocurrent for p-Si/SnO2/SnS2 PD in the presence of (a) 365 nm, the inset showcases magnified I-t curves, (b) 456 nm, (c) 532 nm, (d) 632 nm, and (e) 850 nm wavelengths. (f-j) Corresponding short-circuit currents [absolute transient (It), absolute stable (Is), and relative transient (Itt') currents]. (k-o) and the alterations in responsivity (R) and detectivity (D) correspond to varying illumination intensities.

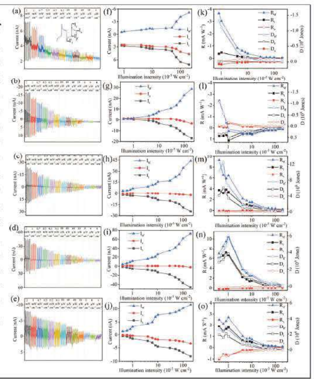

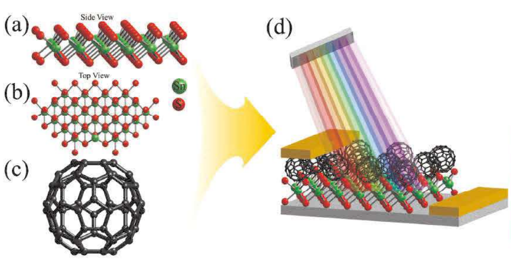

Figure 4. Atomic configuration illustrations. (a, b) Top and side views of SnS_2. (c) Structure of C_{60}. (d) Schematic representation of the C_{60}/SnS_2 heterostructure device.

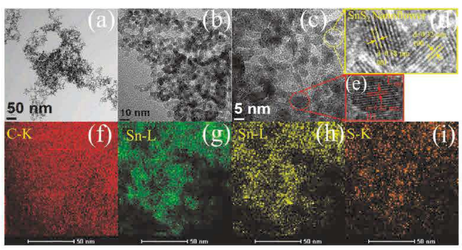

Figure 5. (a-e) TEM and HRTEM images of C_{60}/SnS_2. (f-i) corresponding elemental mappings of C, Sn, and S elements, as indicated.

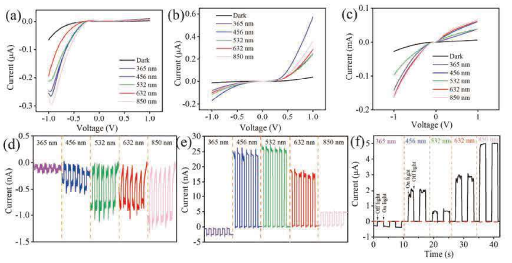

Figure 6. a-c) I-V curves of a) SnS_2 photodetector. b) C_{60} photodetector. c) C_{60}/SnS_2 photodetector under distinct wavelengths. d-f) I-t characteristics of the d) SnS_2 photodetector. e) C_{60} photodetector. f) C_{60}/SnS_2 photodetector under distinct wavelengths.

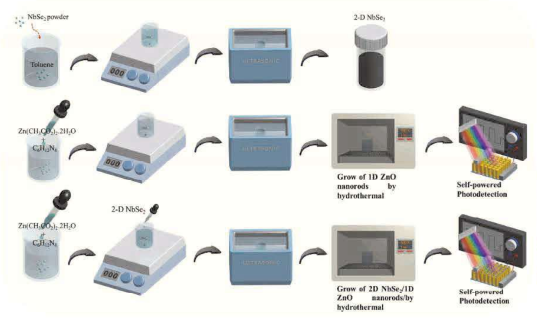

Figure 7. A schematic illustration of the fabrication process for 1D and 2D PDs and their potential use as a self-powered photodetection performance.

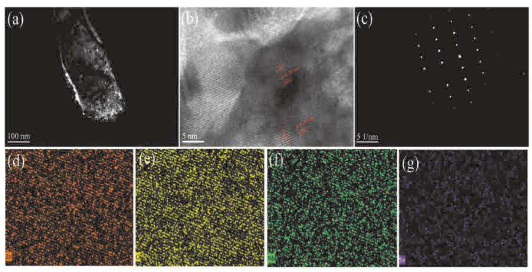

Figure 8. (a) TEM. (b) HRTEM. (c) SAED images of $NbSe_{2(3\ ml)}$-ZNRs. (d–g) corresponding elemental mappings of Zn, O, Nb, and Se elements (as labeled).

Figure 9. Impact of illumination intensities on the short-circuit photocurrent. a–e) short-circuit photocurrent for NbSe2(1 ml)-ZNRs PD. f–j) short-circuit photocurrent for NbSe2(2 ml)-ZNRs PD. k–o) short-circuit photocurrent for NbSe2(3 ml)-ZNRs PD. Under (a,f,k) 365 nm, (b,g,l) 456 nm, (c,h,m) 532 nm, (d,l,n) 632 nm, and (e,j,o) 850 nm wavelengths.

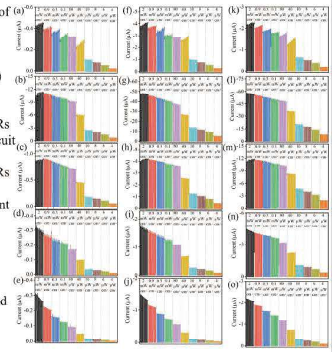

Summary: This research presents significant advancements in hybrid heterostructures for optoelectronic applications, showcasing enhanced transient and pyroelectric currents in 1D SnO_2 nanoneedle/2D SnS_2 nanoflowers, a unique bidirectional photoresponse in 0D C_{60}/2D SnS_2 nanoflowers with wavelength-dependent carrier transport mechanisms, and a 1000-fold improvement in the photo-to-dark current ratio in a 2D $NbSe_2$/1D ZnO nanorod superconductor-semiconductor structure. These innovations pave the way for efficient, self-powered, and broadband photodetectors.

Selected Journal Publications

[1] **M. Kumar**, A. Saravanan, S.C. Chen, B.R. Huang, H. Sun, **Self-powered broadband photosensing through the pyro-phototronic effect in 1D SnO_2 nanoneedles/2D SnS_2 nanoflowers heterostructure**, Appl. Surf. Sci., (2024) 160504, https://doi.org/10.1016/j.apsusc.2024.160504.

[2] **M. Kumar**, B.R. Huang, A. Saravanan, S.C. Chen, W.W.W. Hsiao, H. Sun, **Vertical Hierarchical Architecture of Niobium Diselenide Nanosheets Loaded ZnO Nanorods for High Performance Self-Powered Broadband Photodetection**, Adv. Optical Mater, (2024) 2402370, https://doi.org/10.1002/adom.202402370.

[3] **M. Kumar**, B.R. Huang, A. Saravanan, H. Sun, S.C. Chen, **Self-Powered Broadband Photodetectors Based on Si/SnS_2 and Si/$SnSe_2$ p–n Heterostructures**, Adv. Electron. Mater., (2024) 2400164, https://doi.org/10.1002/aelm.202400164.

[4] **M. Kumar**, A. Saravanan, S.A. Joshi, S.C. Chen, B.R. Huang, H. Sun, **High-performance self-powered UV photodetectors using SnO_2 thin film by reactive magnetron sputtering**, Sens. Actuators A: Phys., 373 (2024) 115441, https://doi.org/10.1016/j.sna.2024.115441.